

Chemical and Magnetic order of FeRh nanoparticles in epitaxy on SrTiO₃ (001)

Véronique Dupuis¹, G. Herrera¹, A. Tamion¹, L. Bardotti¹, D. Le Roy¹ and F. Tournus¹
I. C. Infante², S. Gonzalez², P. Rojo Romeo², B. Vilquin², M. Bugnet⁴,
P. Ohresser³, P. Schoeffmann³, E. Otero³, A. Reyes⁵, A. Vlad⁶, A. Resta⁶, A. Coati⁶.

¹ Institut Lumière Matière, UMR 5306, Univ. Lyon 1-CNRS, F-69622 Villeurbanne Cedex, France.

² Institut des Nanotechnologies de Lyon, CNRS UMR 5270 ECL INSA UCBL CPE, F-69621 Villeurbanne Cedex,

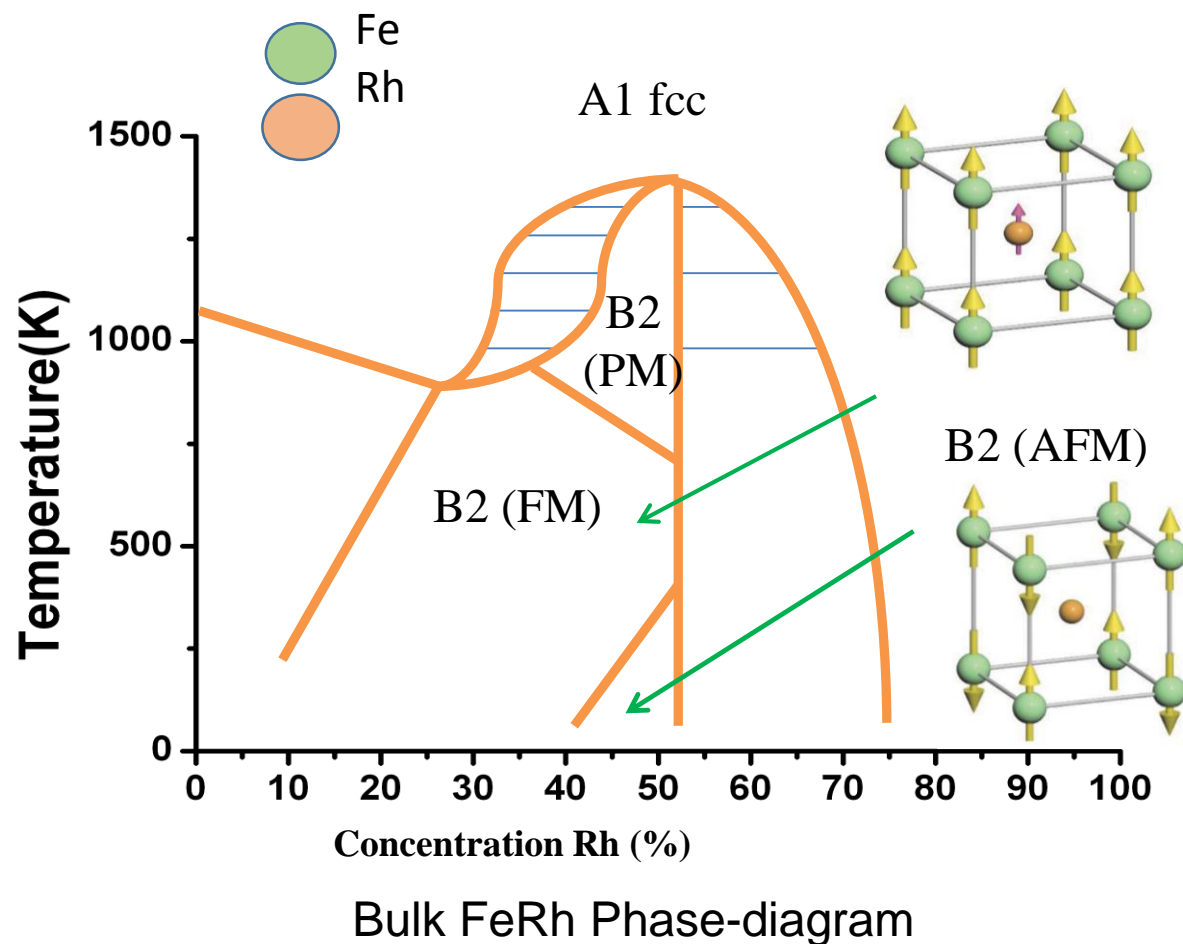
³ DEIMOS-Synchrotron SOLEIL, L'Orme de Merisiers, Saint-Aubin BP 48, F-91192 Gif-sur-Yvette Cedex, France

⁴ MATEIS, UMR 5510, Univ Lyon, CNRS, INSA Lyon, UCBL, 69621 Villeurbanne, France

⁵ Faculty of Science, Universidad Autonoma del Estado de México, Toluca, México.

⁶ SixS-Synchrotron SOLEIL, L'Orme de Merisiers, Saint-Aubin BP 48, F-91192 Gif-sur-Yvette Cedex, France

Chemical and magnetic order in B2 cubic FeRh bulk phase



Metamagnetic transitions in bulk FeRh ($AFM \rightarrow FM \rightarrow PM$)
350 K 650 K

Nano-heterostructure for Multiferroic Refrigeration applications

NATURE COMMUNICATIONS | DOI: 10.1038/ncomms11614

ARTICLE

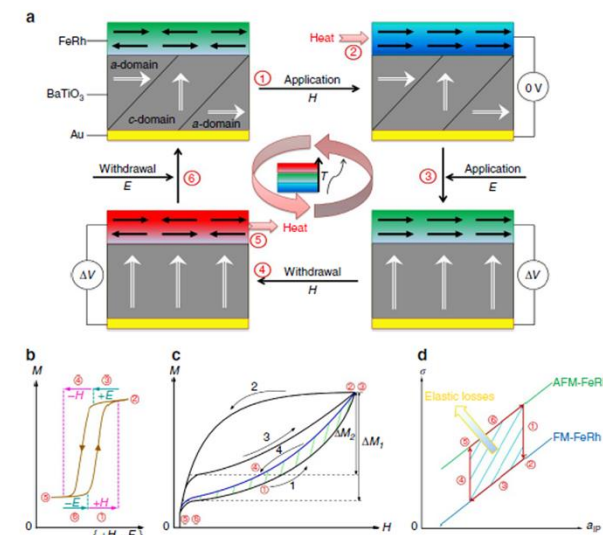


Figure 1 | Multicaloric refrigeration cycle. (a) Schematic of a dual-stimulus multicaloric refrigeration cycle. (b) Schematic of the effect of electric and magnetic fields (E, H) on the magnetization M of FeRh. The electric field overcomes the hysteresis, but does not itself cause M to change. (c) Schematic of magnetic cycles, in the space of magnetization M versus magnetic field H . The blue curve denotes a path followed in the presence of the electric field. Black uncircled numbers refer to measurement paths described in the main text. (d) Schematic of elastic losses, in the space of biaxial thin film stress σ versus average in-plane lattice constant of FeRh a_p . In a-d, the red circled numbers 1-6 correspond to the steps described in the main text, and in b-d arrows indicate the sequence of proposed measurements.

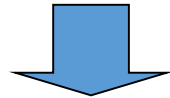
At Nanoscale, chemical order can be obtained by UHV annealing at high T

Structural parameters related to magnetic properties ?

**Platform
PLYRA**

*LECBD Technique :
Low Energy Cluster
Beam Deposition*

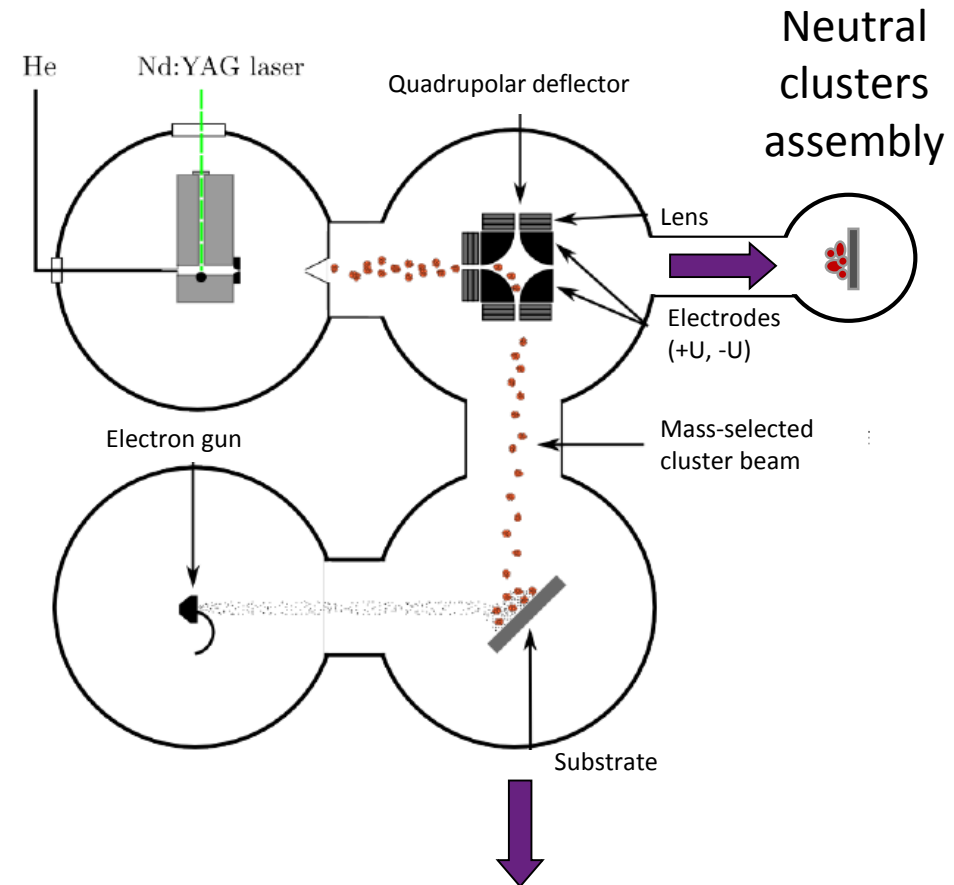
**Laser Vaporisation Source
+ Electrostatic quadrupole**



- Mixed clusters via Target composition
- Random UHV deposition on Surface
- co-deposited Matrix or capping layer
- Coverture rate independent of size

M-S Low energy cluster beam deposition

Deposition under UHV of mass-selected ionized clusters

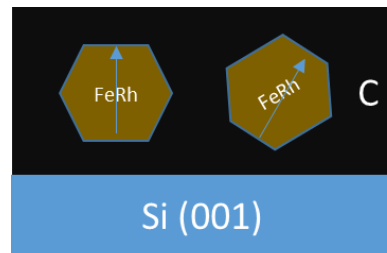


**Soft-landing regime
with narrow size cluster distribution**

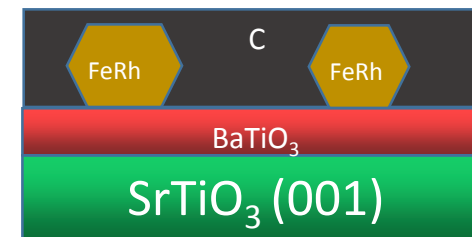
Objectives

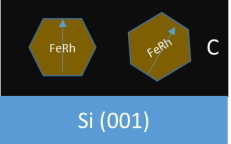
How do the properties of FeRh nanoparticles change when deposited on perovskite substrates?

- Prepare FeRh nanoparticles with 3 nm and 7 nm monomere size
- *In situ* deposited over Si and BTO/STO in UHV + C-capping
- Determine chemical and crystallographic orders.
- Describe magnetic behavior.

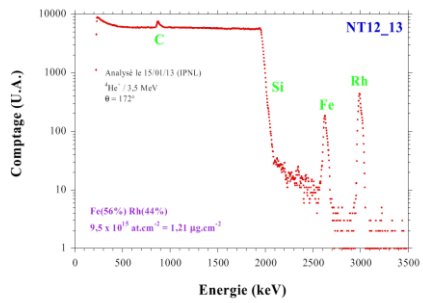


or

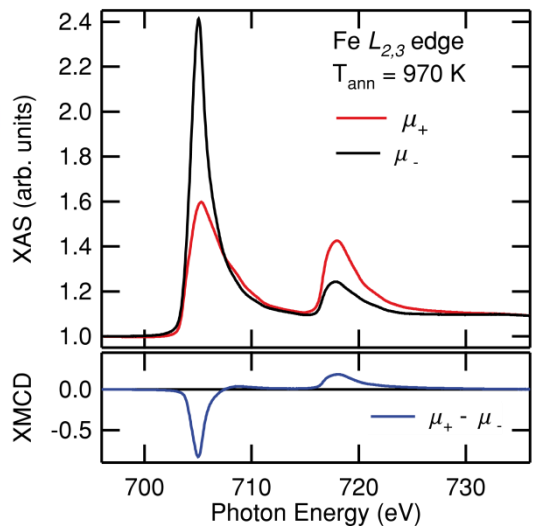
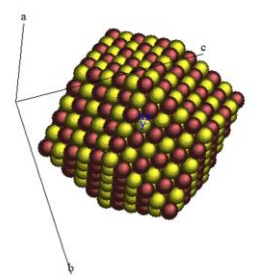
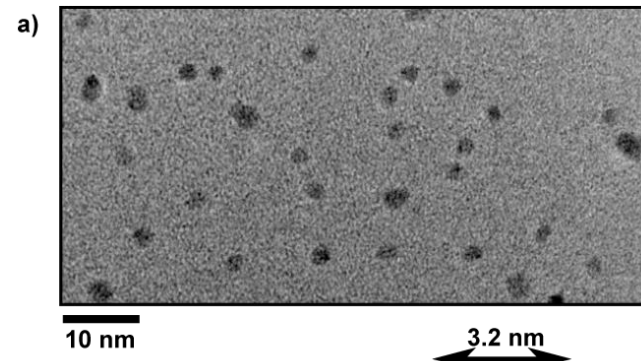




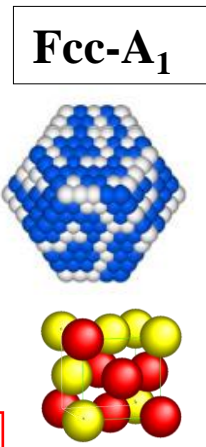
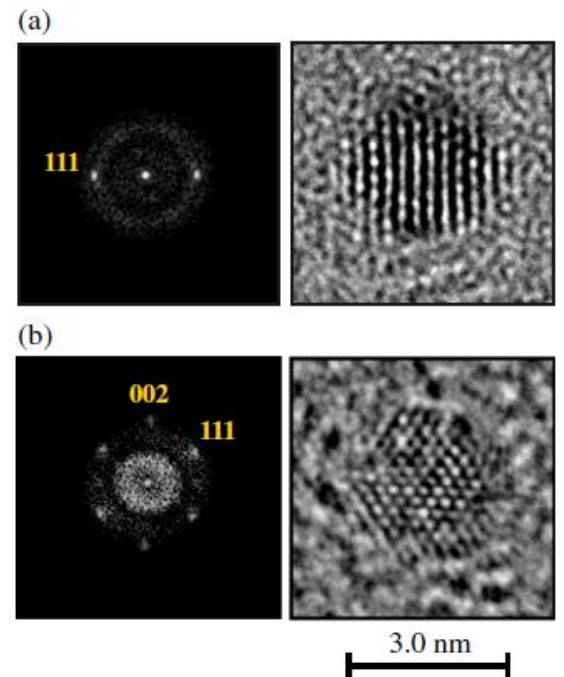
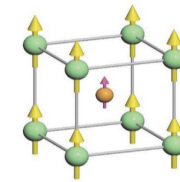
Intrinsic Properties of Mass-selected 3nm-FeRh clusters@C



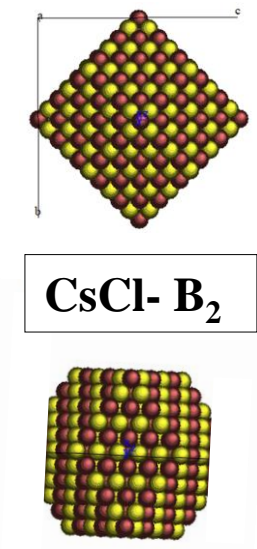
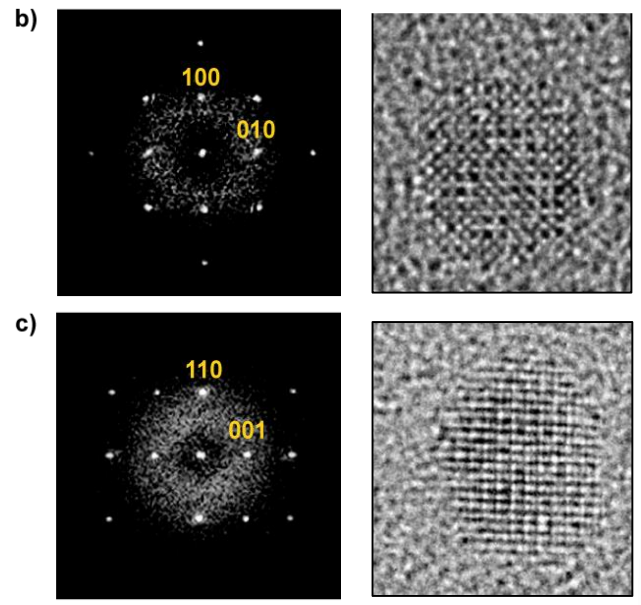
RBS analysis FeRh@C
Fe56%Rh44% ($\pm 5\%$)



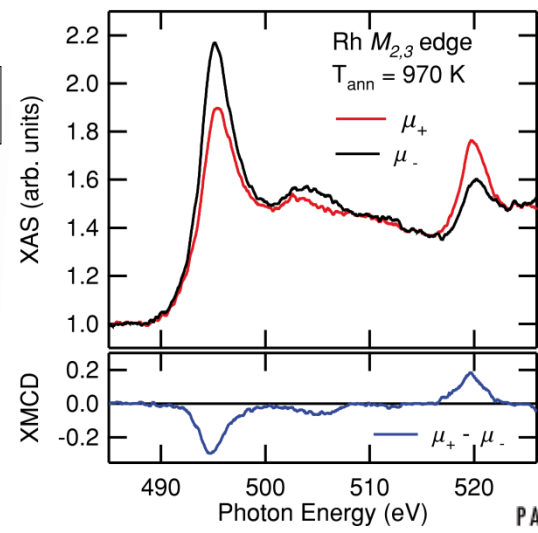
**XMCD at 2K
Fe $L_{2,3}$ edge**



As-prepared FeRh clusters



Annealed 3nm-FeRh clusters



**... But FM from
2K - 350 K**

Rh $M_{2,3}$ edge

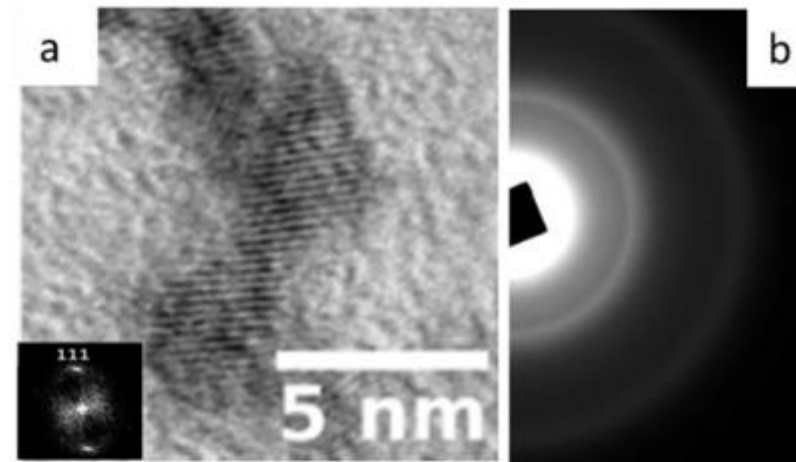
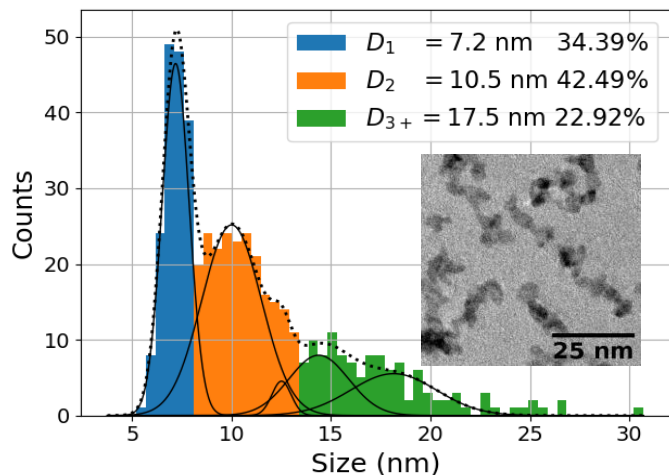
CS HRTEM, Coll. K. Sato, Sendai Japan

Fcc- A1 chemically disordered \rightarrow Cubic B2 chemically ordered FeRh NPs ...



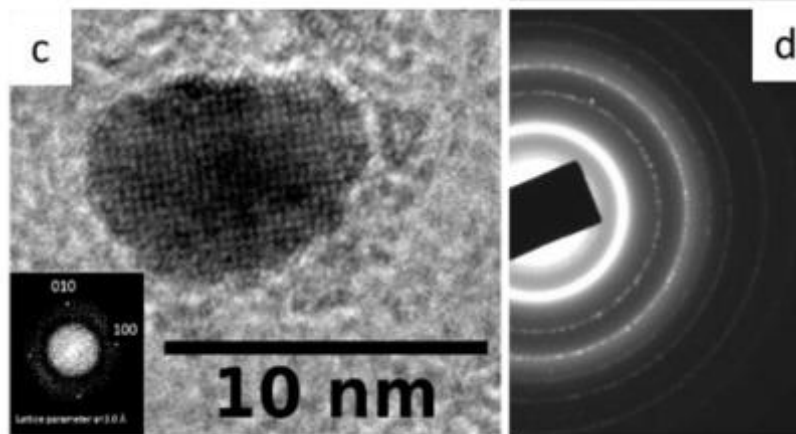
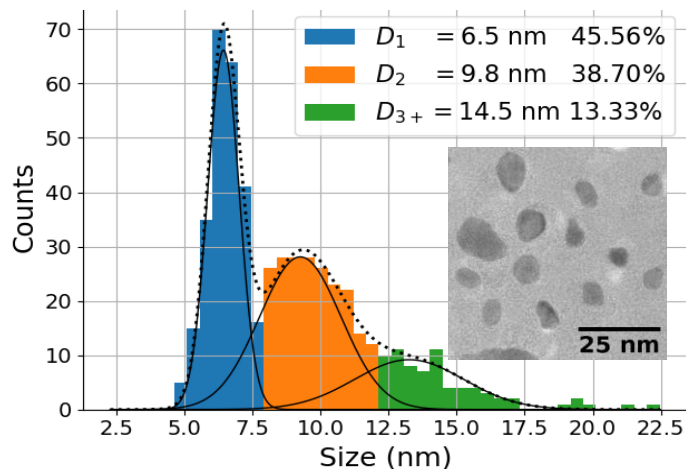
- FeRh nanoparticles of 7 nm (nominal monomer size on TEM grid)
- After annealing, nanoparticles are in B2 phase and become rounder.

As prepared



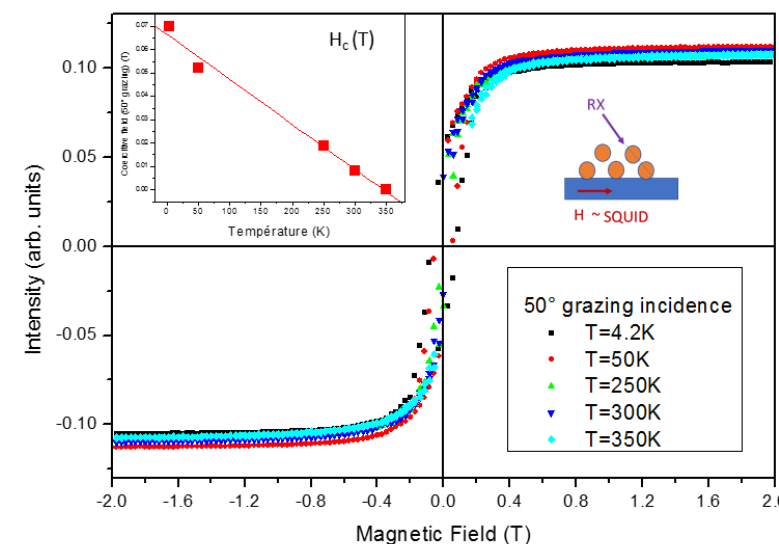
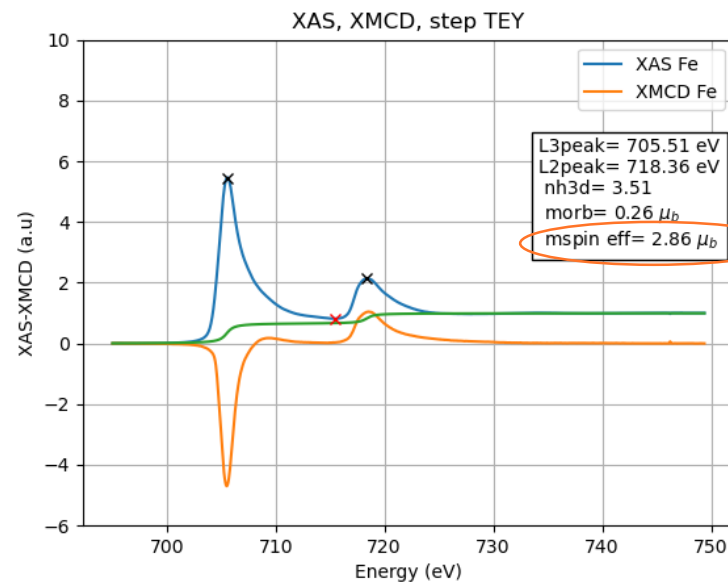
A1 FeRh
FCC

Annealed at 700 °C

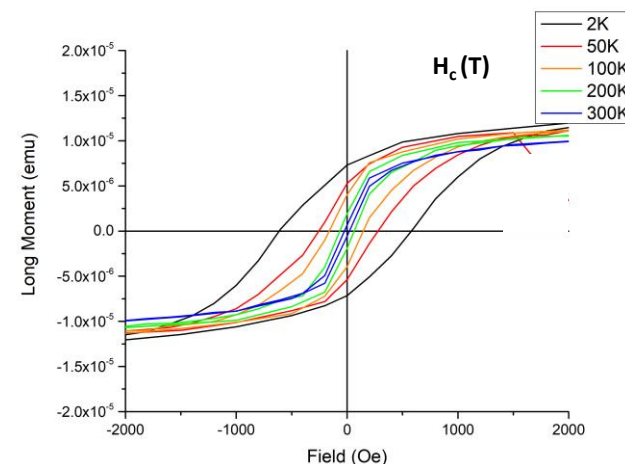
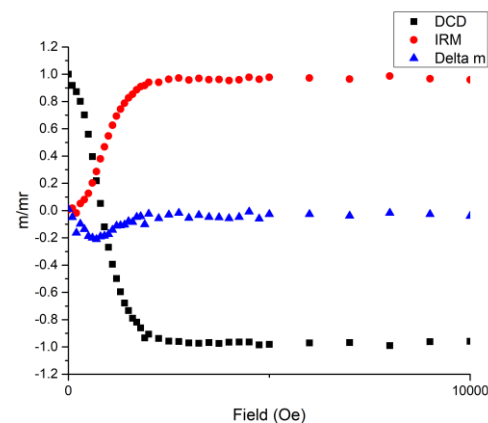


B2 FeRh
cubic

XMCD at 4.2K at Fe $L_{2,3}$ edge on annealed 7nm-FeRh B2 clusters@C on Si at DEIMOS



In agreement with SQUID magnetometry: FM behaviours up at 2K for moderate NPs interaction



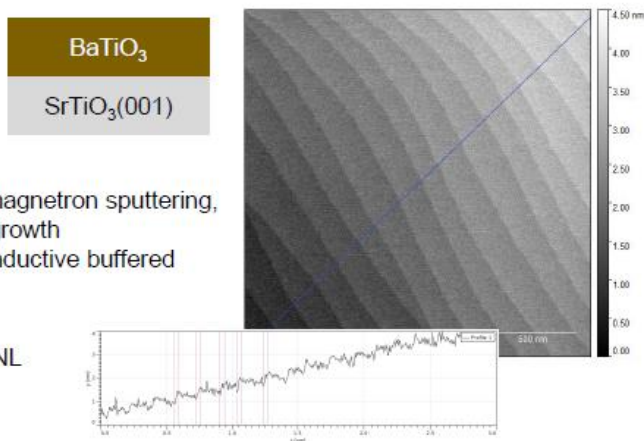
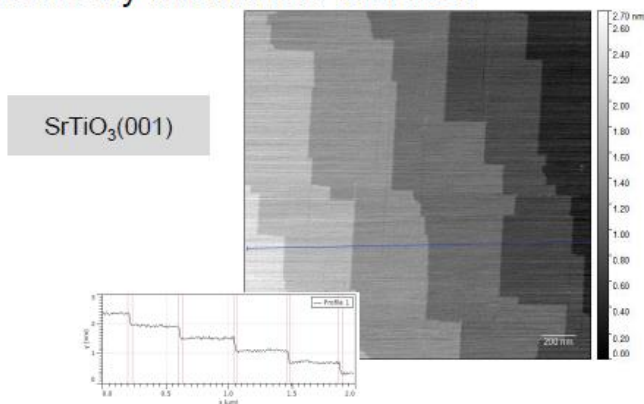
Ferromagnetic order at Low T for B2 FeRh NPs up to 10 nm in diameter !



Mass-selected FeRh clusters deposited on perovskite oxide

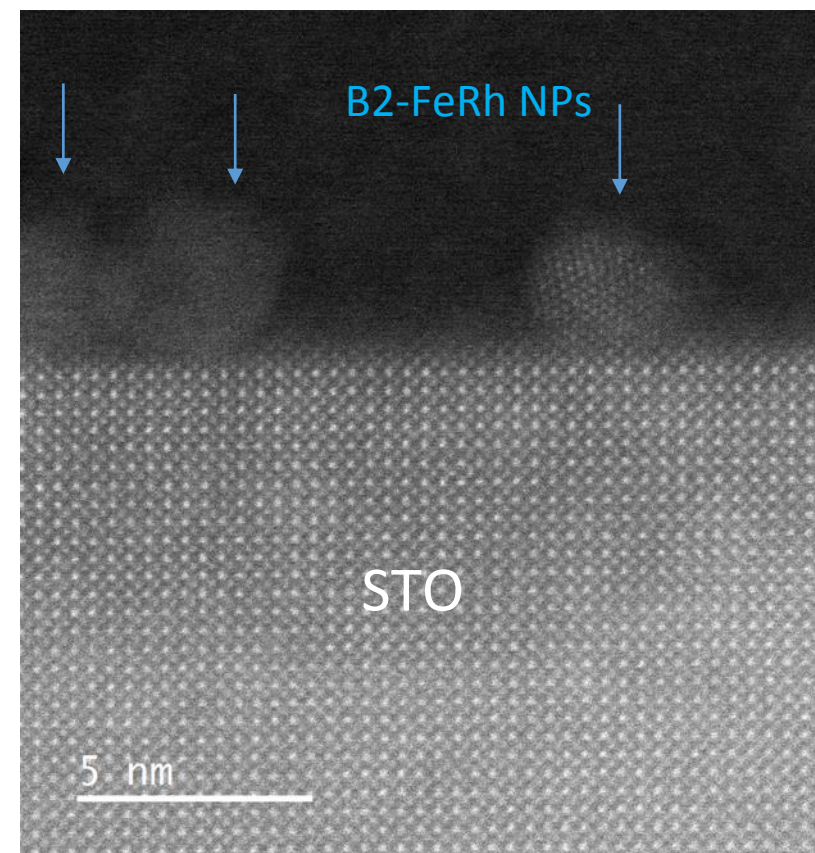
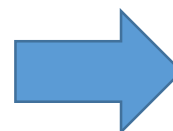
SrTiO₃, BaTiO₃ films (001) @INL

Atomically flat titanate surfaces



BaTiO₃: Radio-frequency magnetron sputtering, high temperature, thin film growth
Different substrates and conductive buffered substrates under study

Atomic Force Microscopy, INL



STEM HAADF, CLYM St Etienne

VOLtage CONtrol of NANOmagnet

ANR-19-CE09-0023

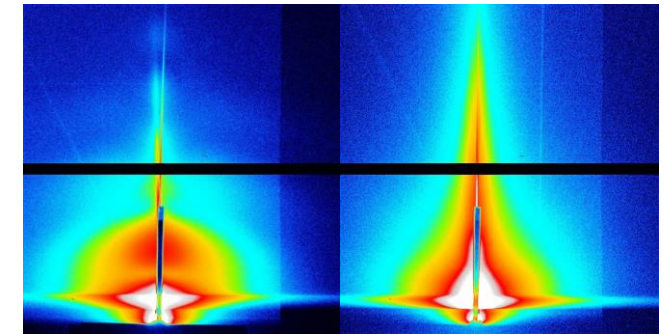
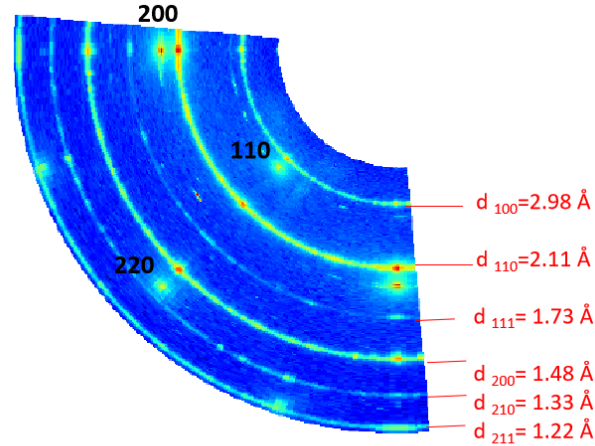
B2 FeRh NPs on perovskite substrate

at BM32-ESRF
beamline

In situ UHV annealed 2C/FeRh 3 nm monomer/SrTiO₃



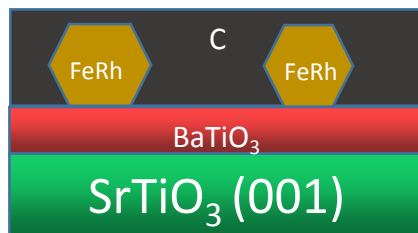
FeRh[110] / SrTiO₃[020]



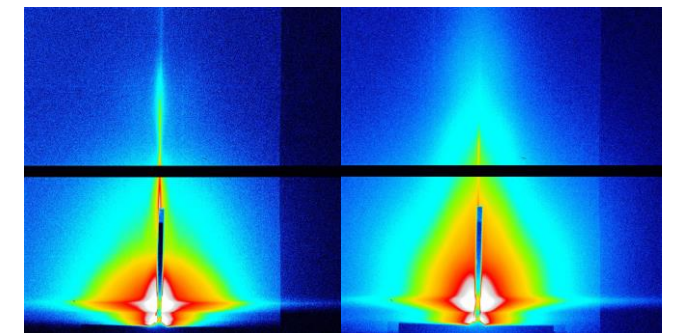
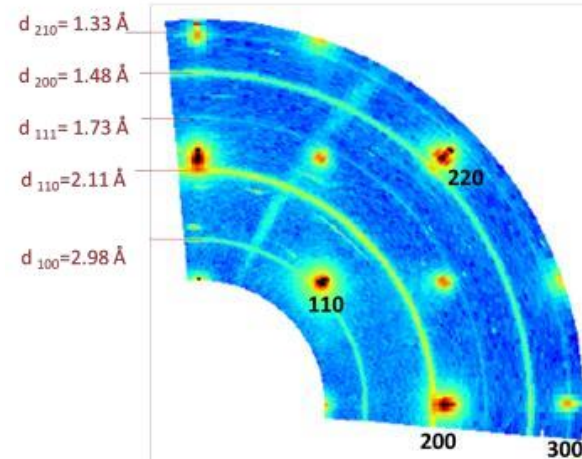
as prepared

700 °C

In situ UHV annealed 2C/FeRh 7 nm monomer/thin BaTiO₃/SrTiO₃

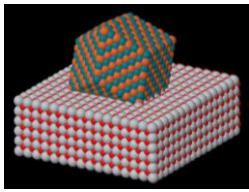


FeRh[110] / thin
BaTiO₃[020] on STO



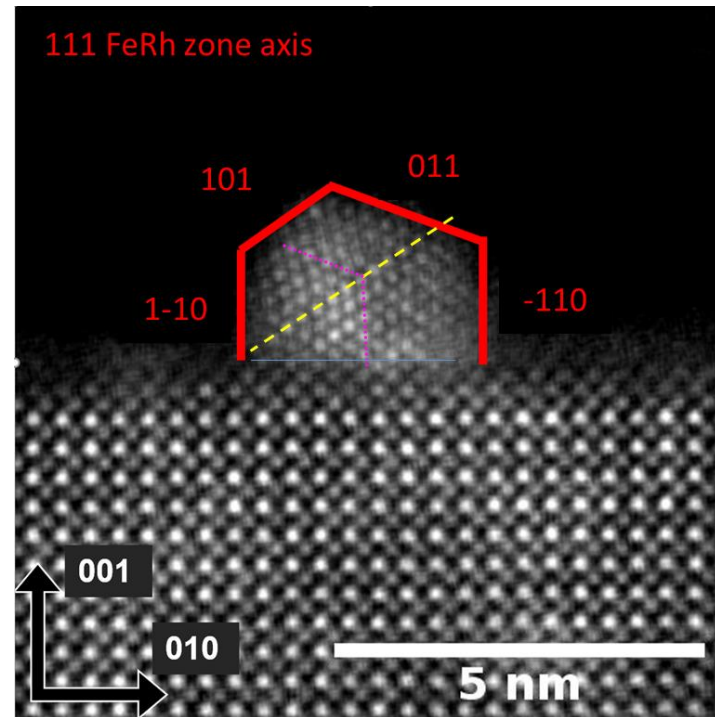
as prepared

700 °C



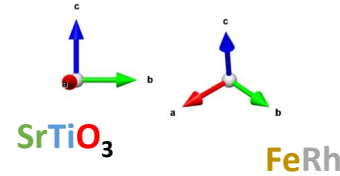
STEM-HAADF @ 200 kV
(Cs-corrected Jeol NeoARM)
Cross-section sample by FIB

B2 FeRh NPs on perovskite evidence of several Epitaxies



Epitaxy FeRh [1-10]/SrTiO₃[100]
seen by STEM and GIXRD

New epitaxy (1)
[1-10] FeRh // [100] SrTiO₃
[111] FeRh // [010] SrTiO₃



→ (11-2) FeRh plane contact
Anisotropic in-plane strain

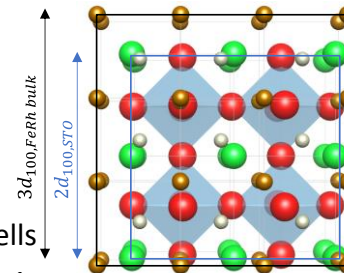
$$\epsilon_{1-10/100} = \frac{d_{100,STO} - 2d_{1-10,FeRh\ bulk}}{2d_{1-10,FeRh\ bulk}} = -7.42\%$$

New epitaxy (2)
[100] FeRh // [100] SrTiO₃
[110] FeRh // [110] SrTiO₃

→ (001) FeRh plane contact

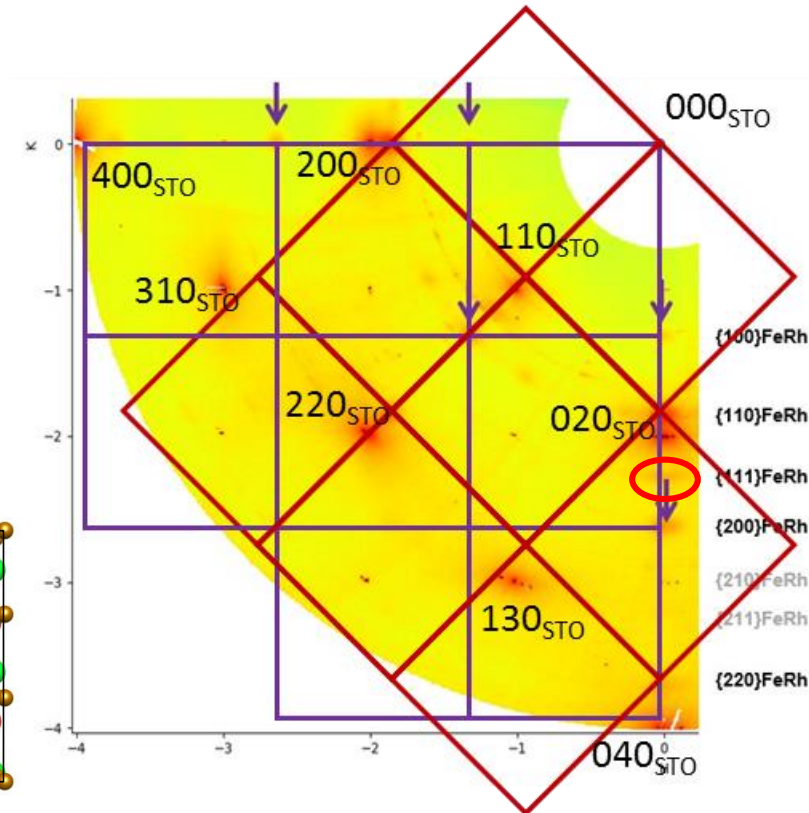
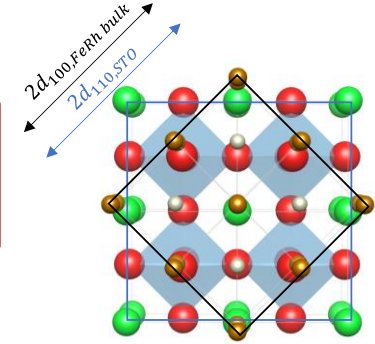
3 FeRh cells cube-on-cube on 2 SrTiO₃ cells

$$\epsilon_{100/100} = \frac{2d_{100,STO} - 3a_{FeRh\ bulk}}{3a_{FeRh\ bulk}} = -12.73\%$$



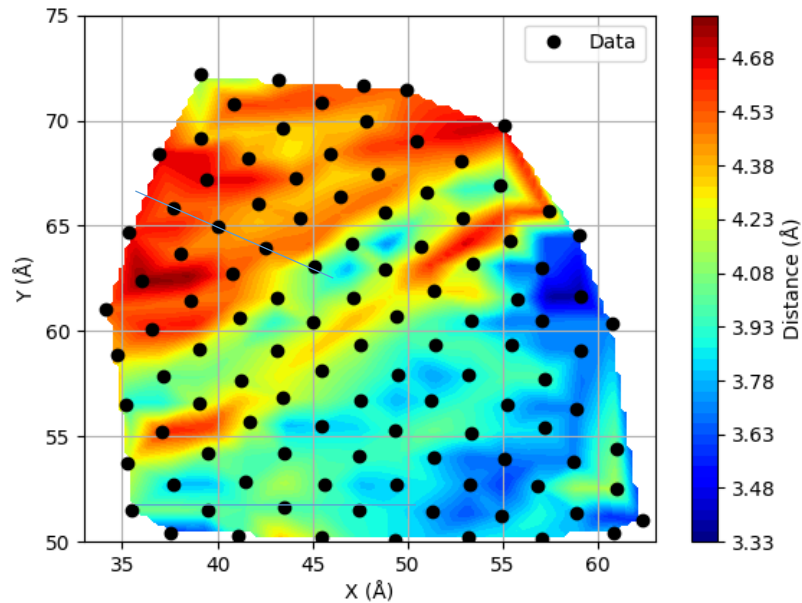
Conventional epitaxy
[110] FeRh // [100] SrTiO₃
[1-10] FeRh // [010] SrTiO₃

→ (001) FeRh plane contact
FeRh cell axes at 45°



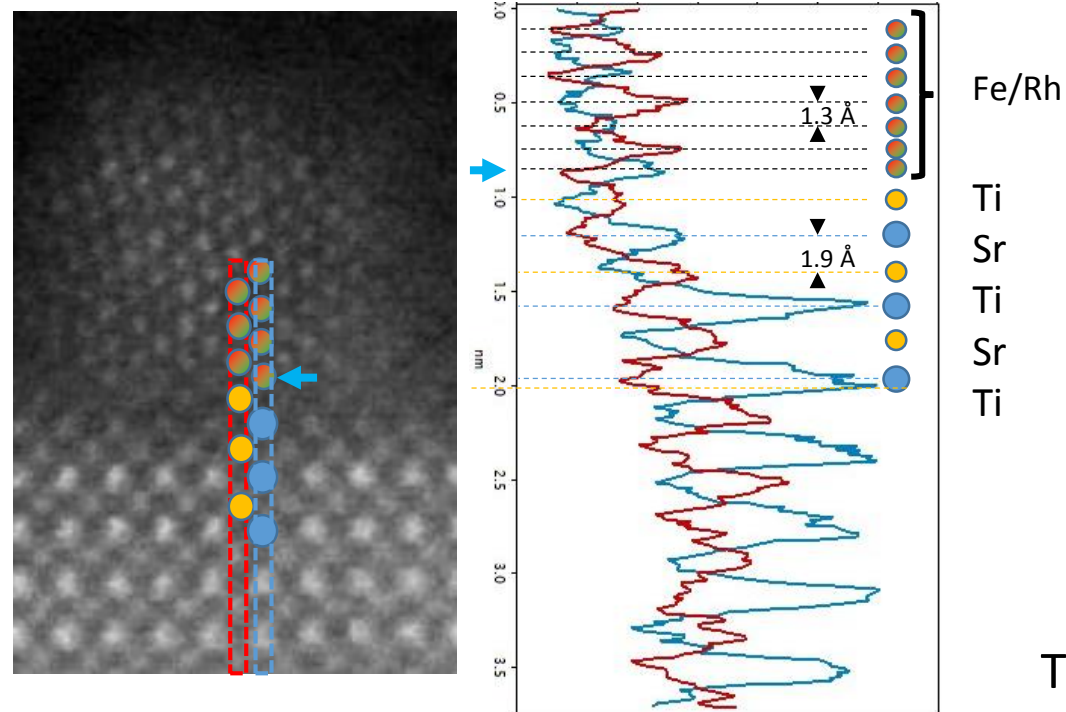
Single B2 FeRh NP on STO substrate

STEM-HAADF @ 200 kV
(Cs-corrected Jeol NeoARM)
Cross-section sample by FIB



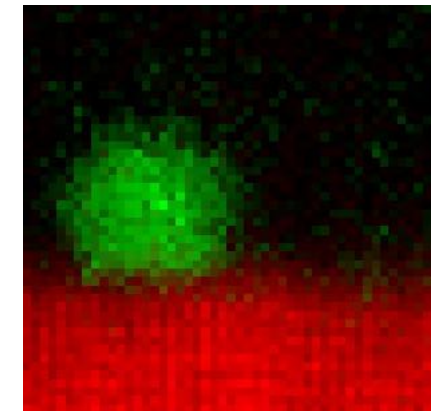
- Is possible to identify positions.
- Possible twinning and deformation.
- Epitaxy at the interface.

STEM-HAADF



SrTiO₃ (001) surface is Ti terminated

STEM-EELS



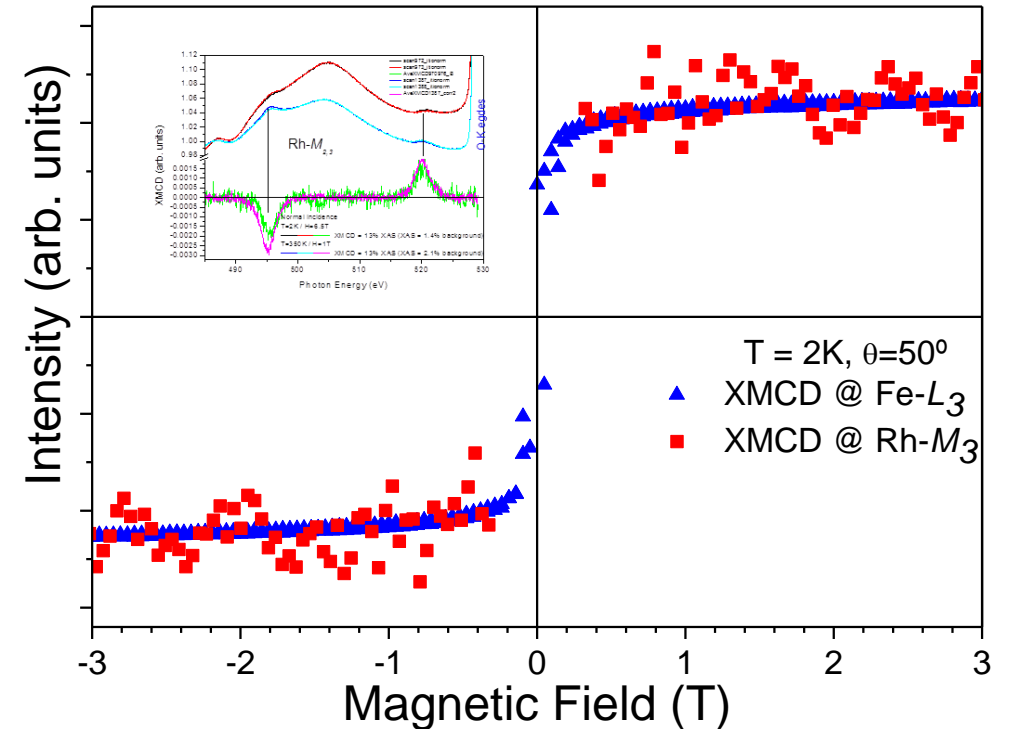
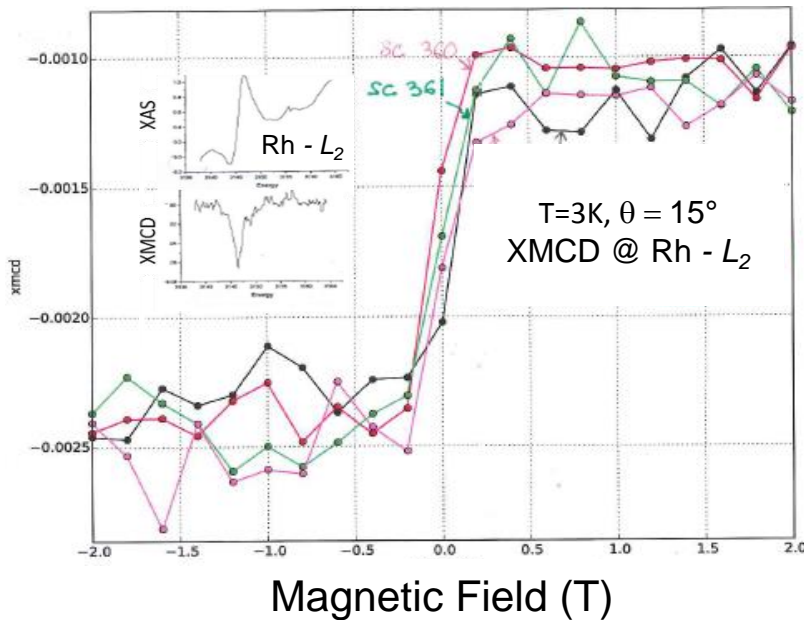
Fe-L₂₃, Ti-L₂₃

There is no diffusion of Ti or Fe

Sharp Interface and strain
→ (11-2) FeRh plane contact
Anisotropic in-plane strain

Magnetic Properties of B2 FeRh NPs on perovskite

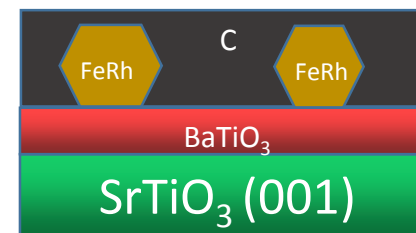
XMCD at Rh-L edge (ID12 –ESRF) and at Fe-L and Rh-M edges (DEIMOS –SOLEIL)



➤ Strong FM coupling between Fe and Rh moment even at low temperature

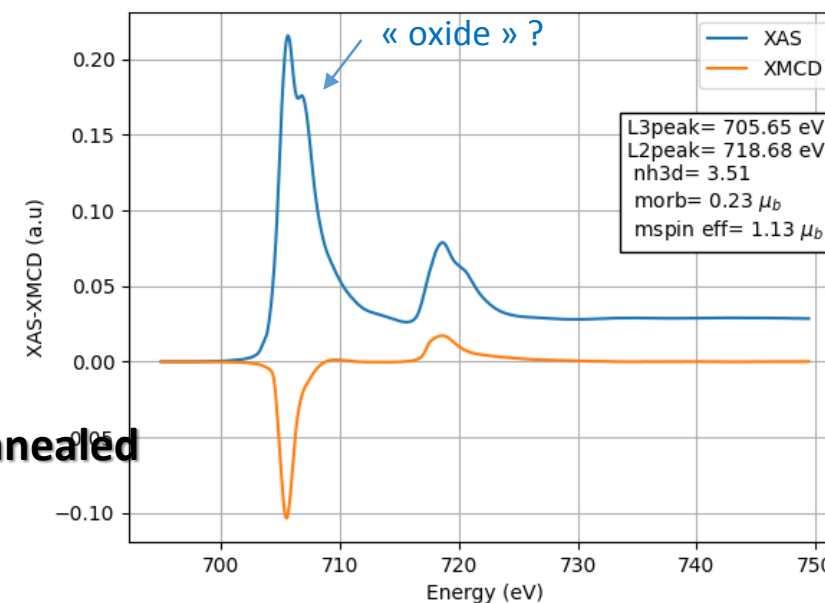
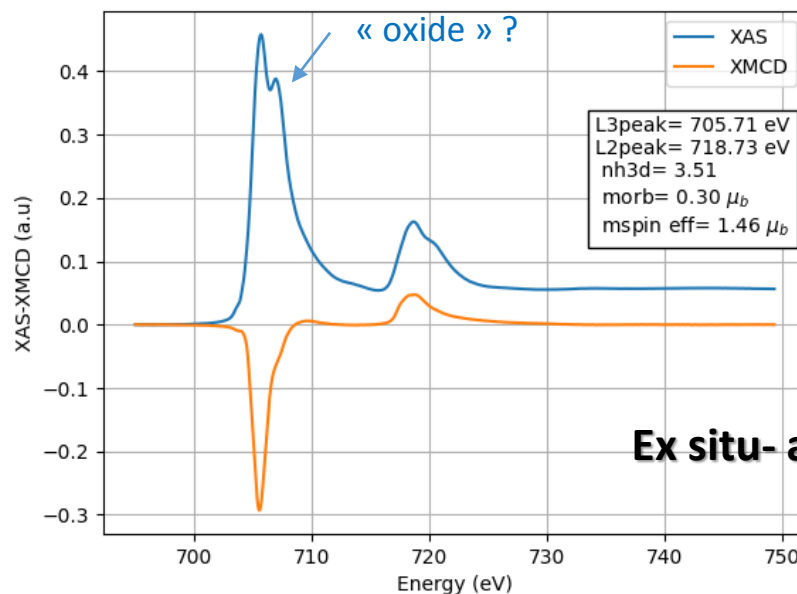
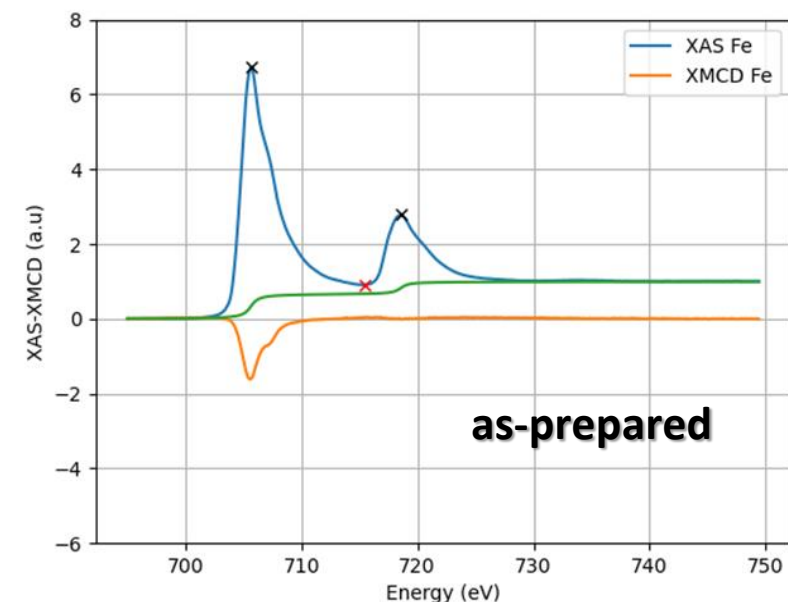
Magnetic Properties of B2 FeRh NPs on perovskite

As-prepared and UHV annealed sample avec C-capping :
2C/FeRh 7 nm monomer/BaTiO₃/SrTiO₃



XMCD at Fe-L_{2,3} edge @ 2 K

@ 350 K



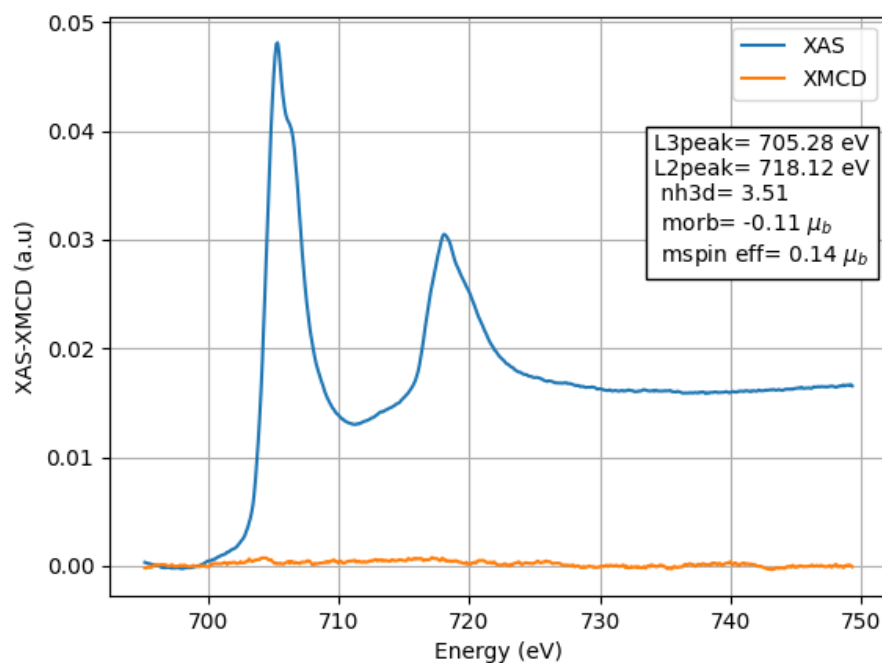
Magnetic Properties of B2 FeRh NPs on perovskite

Deoxidation of FeRh NPs possible from :

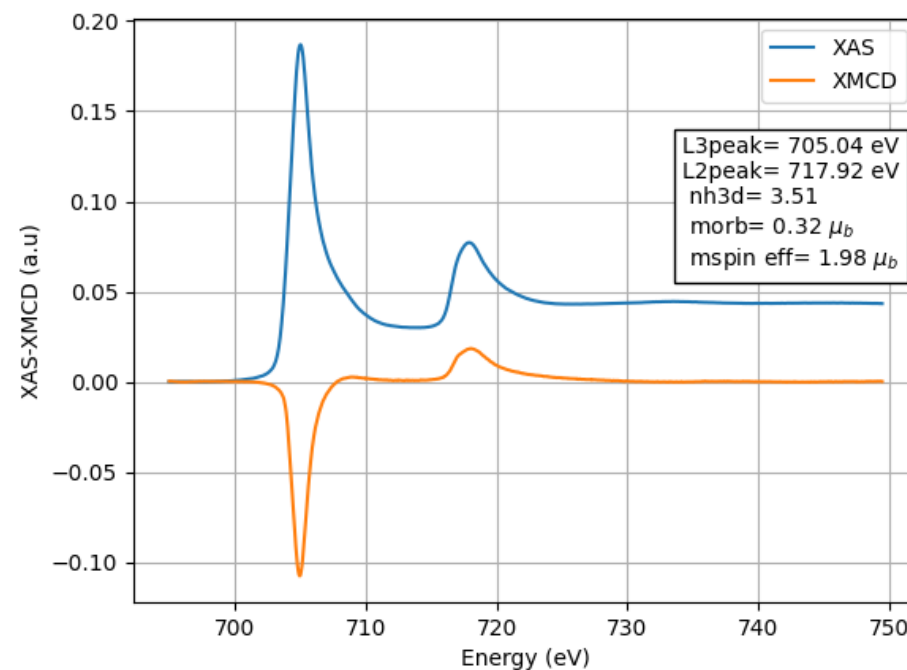
In situ UHV annealing FeRh 3 nm monomer/SrTiO₃
ms is reduced compared to same sample on Si : Fe magnetic dead layer on STO ?



Sample as prepared

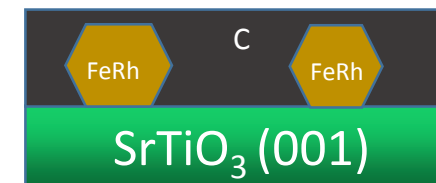


Sample *in situ* annealed 600°C

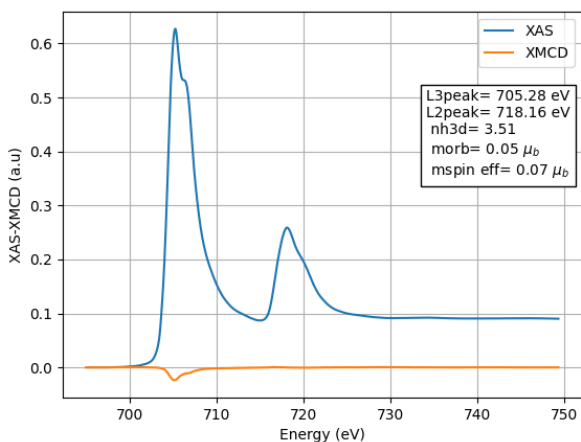


Magnetic Properties of B2 FeRh NPs on perovskite

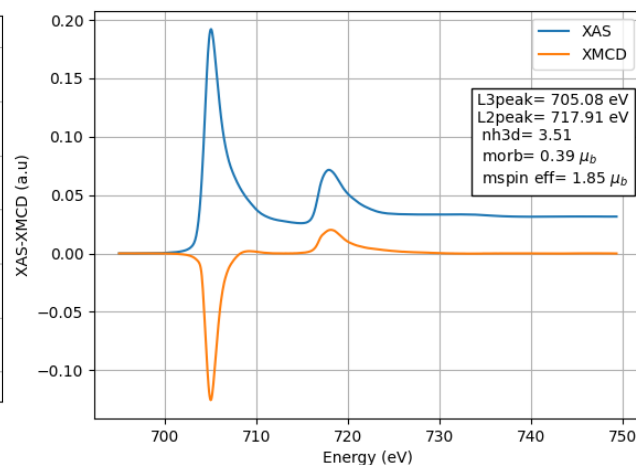
Deoxidation of FeRh NPs on STO



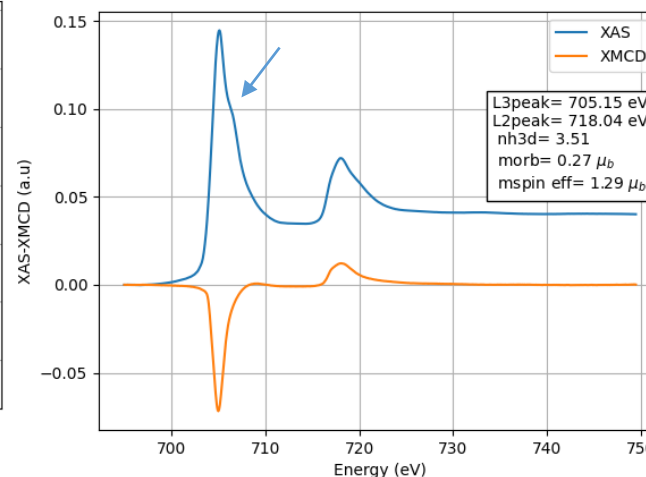
Sample
as-prepared



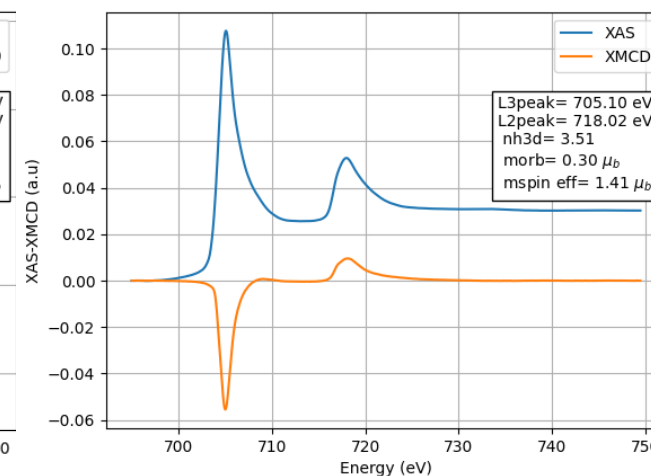
in situ UHV annealed
up to 800°C



after transfer in air
(after 2 months)



in situ UHV reduced
at 500°C



In situ UHV annealing FeRh 3 nm monomer/SrTiO₃
But *ms* reduced (magnetic dead layer on STO ?)

Conclusion on chemically ordered FeRh NPs over Perovskite oxides

- B2-FeRh nanoparticles present several **epitaxy over SrTiO_3 and thin BaTiO_3**
- with **strong** Lattice parameter **strain**
- FeRh NPs get partially oxidized, but **can be deoxidized from in situ annealing at 600°C .**
- **No migration of Fe or Ti at Interface.**
- **Relaxation and size effect** still present on avoiding **AntiFerromagnetic** state at low temperature



VOLtage CONTROL of NANOmagnet

ANR-19-CE09-0023

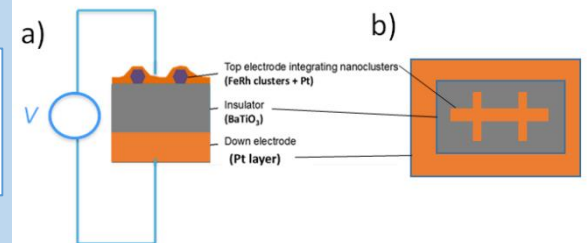


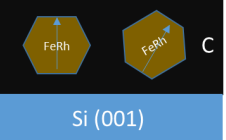
Figure: (a) Side and (b) top views of the multiferroic

Acknowledgment

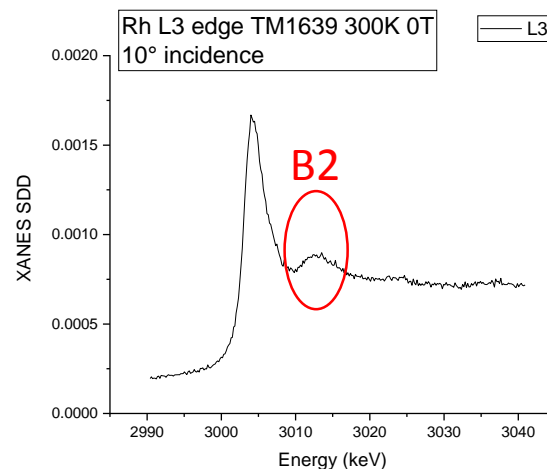
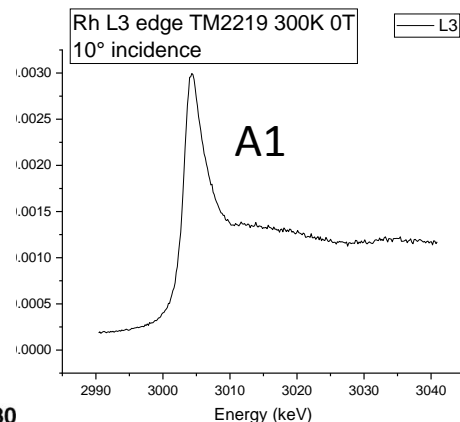
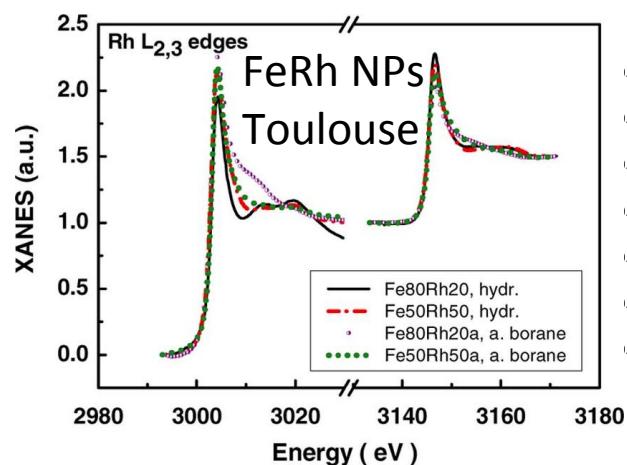
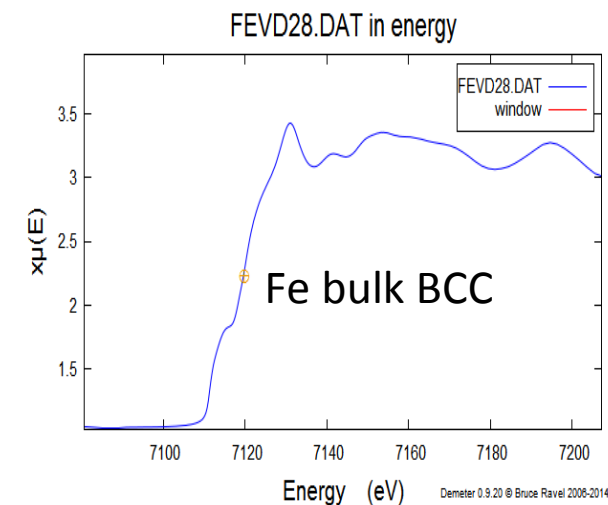
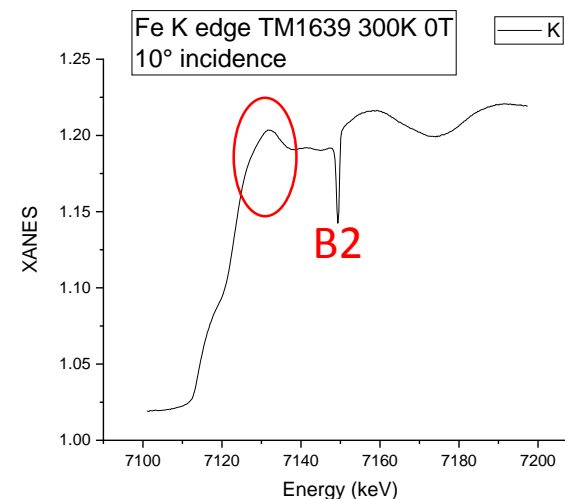
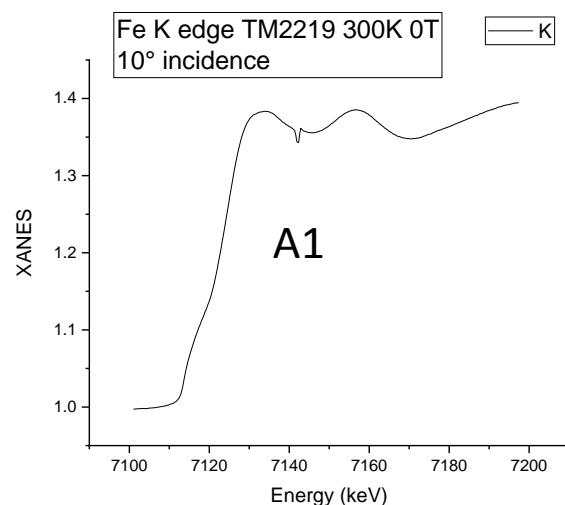
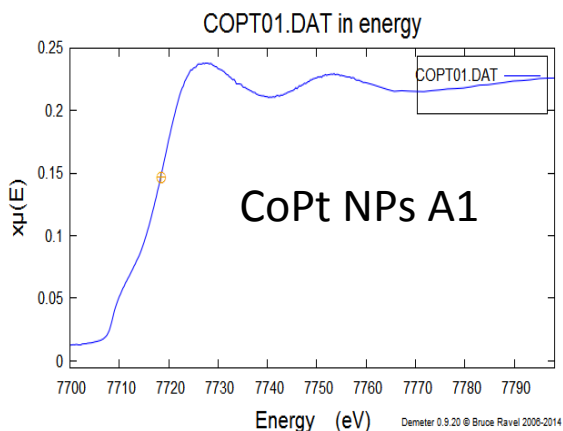
- ANR project VOLCONANO
- DEIMOS-SOLEIL Synchrotron
- SIXS-SOLEIL Synchrotron
- BM32-ESRF Synchrotron
- ID12-ESRF Synchrotron
- CLYM







XANES thin Mass-selected 7nm-FeRh@ C samples / Si

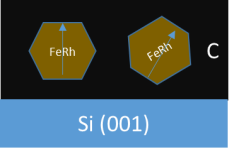


Rh L₂-edge

at ID12 - ESRF beamline

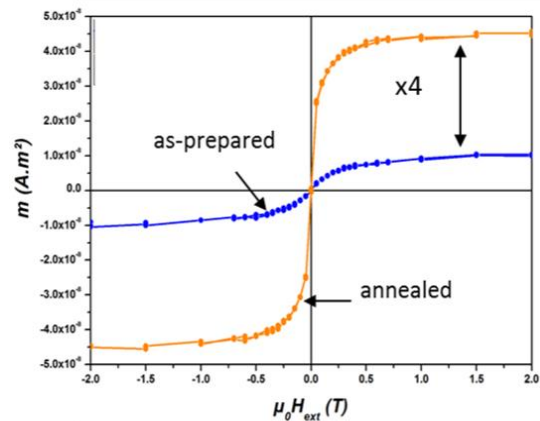


as-prepared / annealed

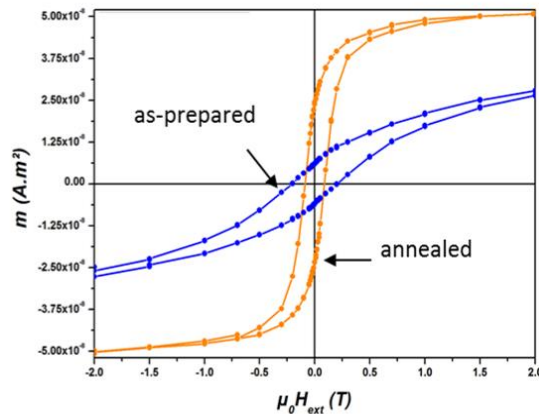


SQUID on Mass-selected 7nm-FeRh@ C / Si

Low density : 4 %

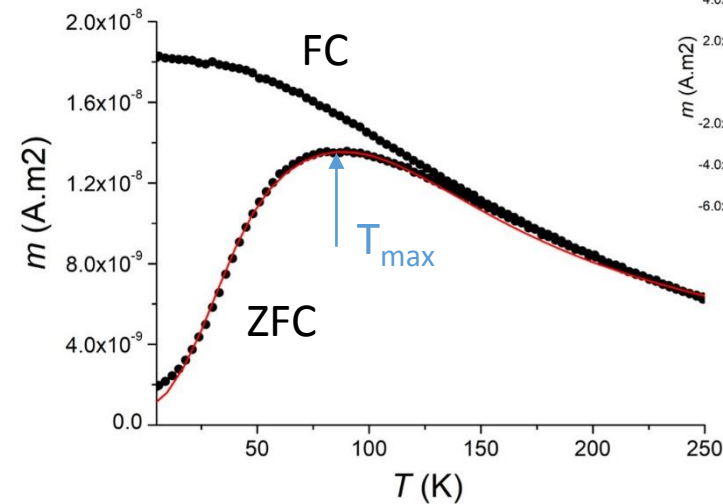


SP @100 K



FM @ 2 K

TM 16-39 FeRh environ 4 %



$Dm1 = 6.3 \text{ nm}$
 $w = 0.08$
 74 % de monomère (fixé par rapport au TEM)
 $Dm2 = 1.26 * Dm1$
 $w2 = 0.08$
 $K1 = 123 \text{ kJ/m}^3$
 $wK1 = 0.38$;
 il y a une large distribution de constante d'anisotropie
 (comme pour le Co)

ZFC/FC susceptibility and Hysteresis loops @ 300 K
for annealed sample

➤ No Metamagnetic transition for annealed thin mass-selected FeRh @ C with 7 nm in diameter

Large mass-selected FeRh sample @ C, Guillermo Herrera et al. EPJAP (2022)

FeRh / STO epitaxy : details

Epitaxial relationships

Lattice mismatch, cell matching

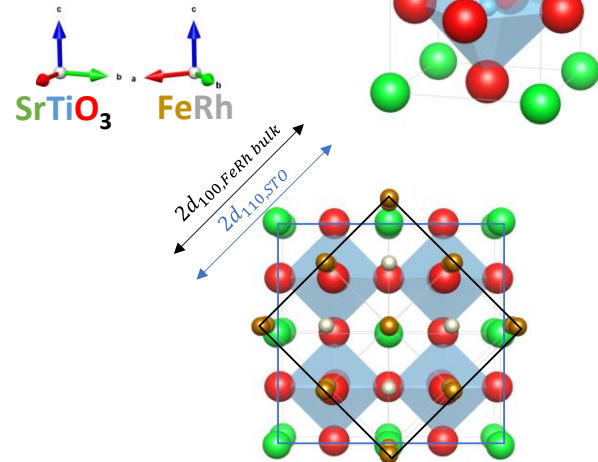
Conventional epitaxy

[110] FeRh // [100] SrTiO₃

[1-10] FeRh // [010] SrTiO₃

→ (001) FeRh plane contact
FeRh cell axes @ 45deg from SrTiO₃ ones

$$\epsilon_{110/100} = \frac{2d_{110,STO} - 2d_{100,FeRh\ bulk}}{2d_{100,FeRh\ bulk}} = -7.43\%$$



New epitaxy (1)

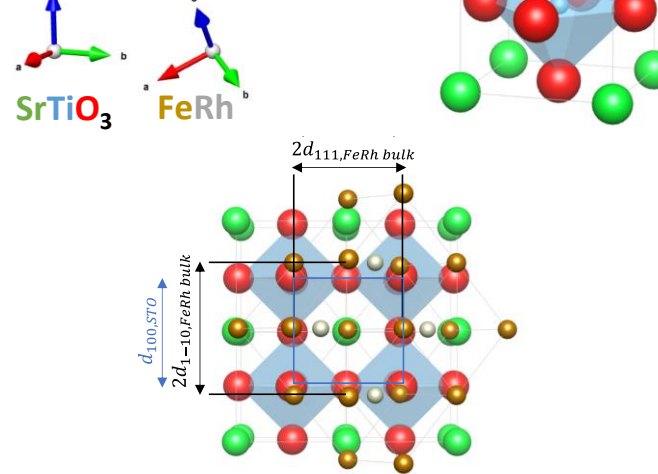
[1-10] FeRh // [100] SrTiO₃

[111] FeRh // [010] SrTiO₃

→ (11-2) FeRh plane contact
Anisotropic in-plane strain

$$\epsilon_{1-10/100} = \frac{d_{100,STO} - 2d_{1-10,FeRh\ bulk}}{2d_{1-10,FeRh\ bulk}} = -7.42\%$$

$$\epsilon_{111/010} = \frac{d_{010,STO} - 2d_{111,FeRh\ bulk}}{2d_{111,FeRh\ bulk}} = +13.39\%$$



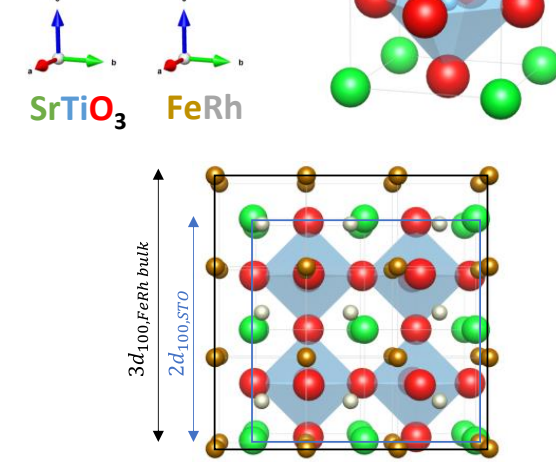
New epitaxy (2)

[100] FeRh // [100] SrTiO₃

[110] FeRh // [110] SrTiO₃

→ (001) FeRh plane contact
3 FeRh cells cube-on-cube on 2 SrTiO₃ cells

$$\epsilon_{100/100} = \frac{2d_{100,STO} - 3a_{FeRh\ bulk}}{3a_{FeRh\ bulk}} = -12.73\%$$



Under large lattice mismatch: unusual epitaxies can be stabilized in small volume objects, *ie* NCs

Bulk crystals

FeRh B2 phase, Pm-3m, a = 2.983Å

SrTiO₃ Pm-3m, a = 3.905Å

FeRh / STO epitaxy : STEM-HAADF

Epitaxial relationships

Lattice mismatch, cell matching

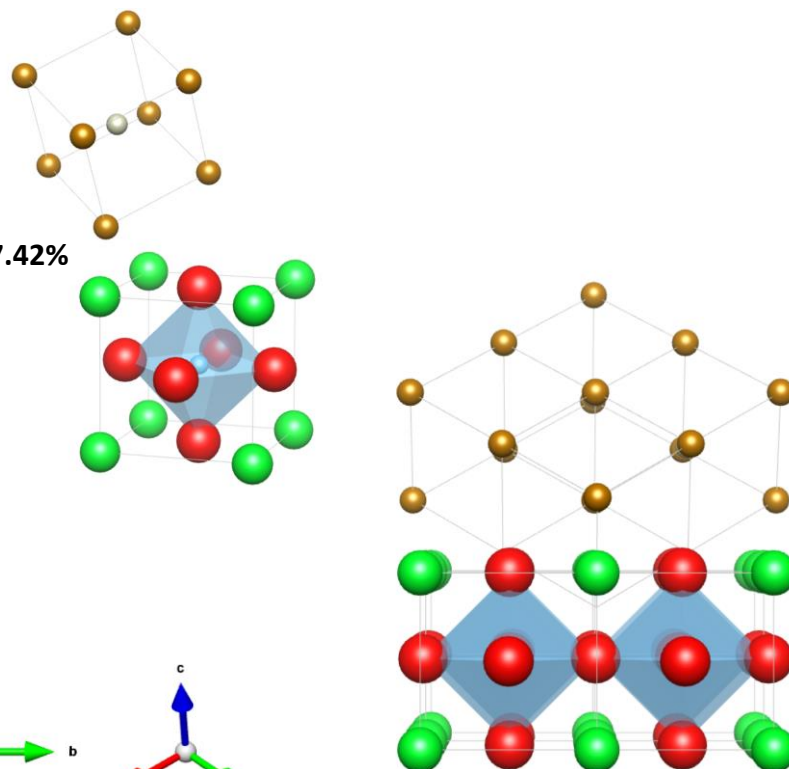
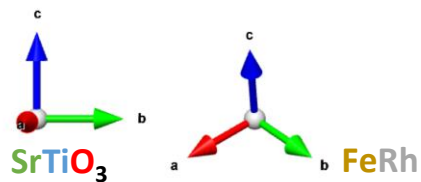
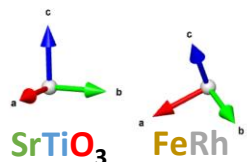
New epitaxy (1)

[1-10] **FeRh** // [100] **SrTiO₃**

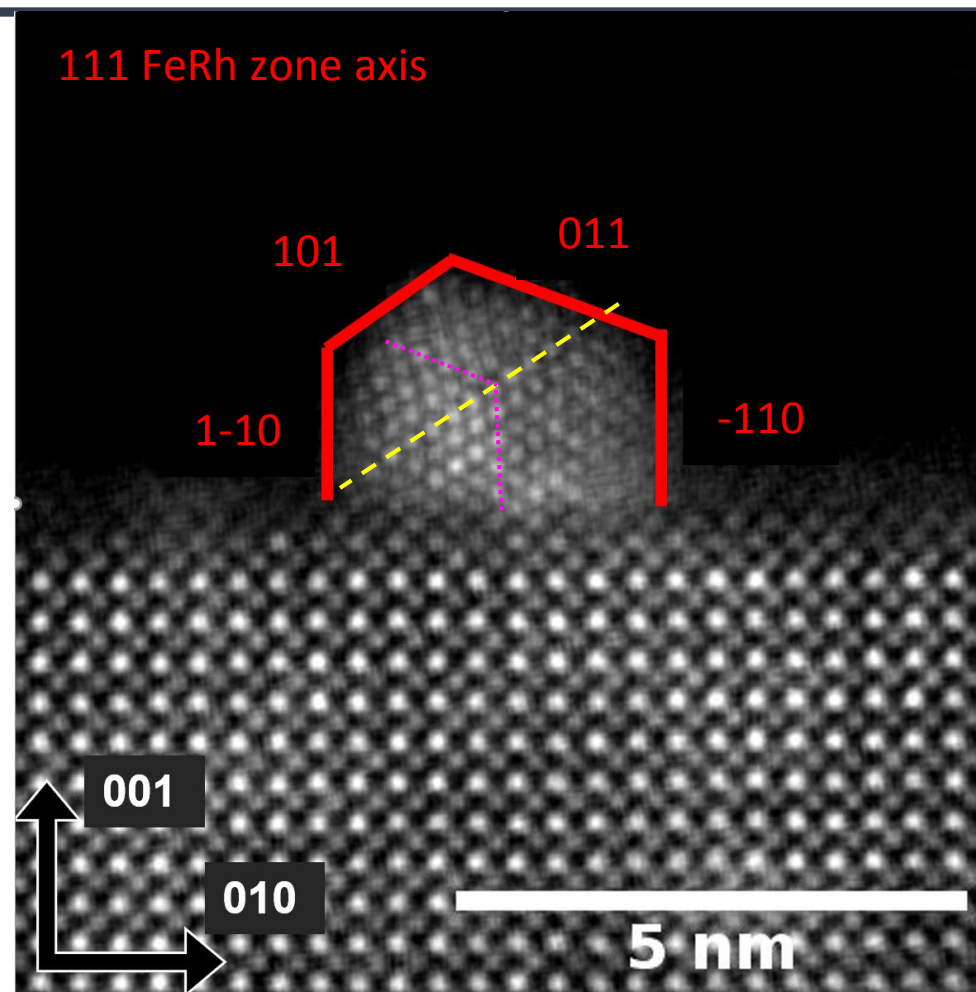
[111] **FeRh** // [010] **SrTiO₃**

→ (11-2) FeRh plane contact
Anisotropic in-plane strain

$$\epsilon_{1-10/100} = \frac{d_{100,STO} - 2d_{1-10,FeRh \text{ bulk}}}{2d_{1-10,FeRh \text{ bulk}}} = -7.42\%$$



STEM HAADF
New epitaxy (1)

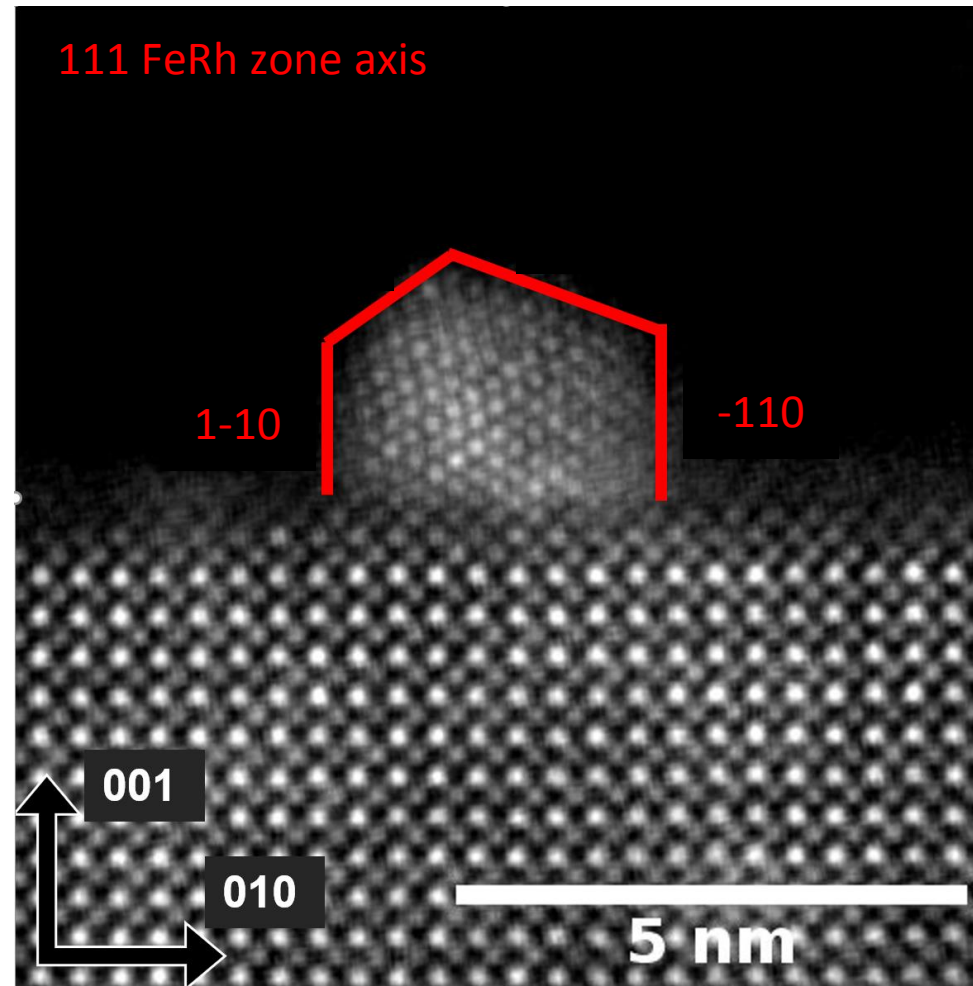


Under large lattice mismatch: unusual epitaxies can be stabilized in small volume objects, *ie* NCs

Bulk crystals

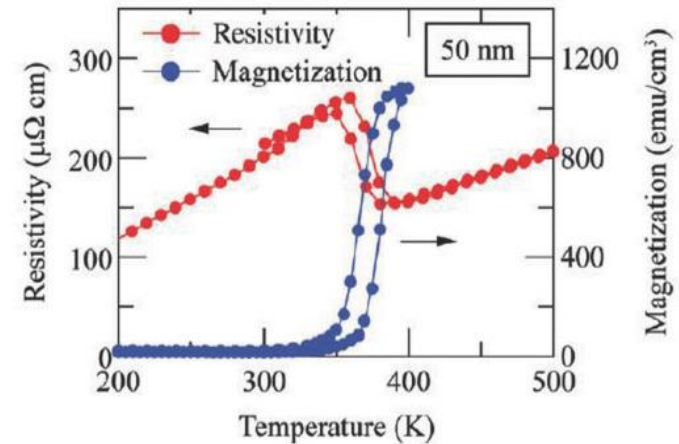
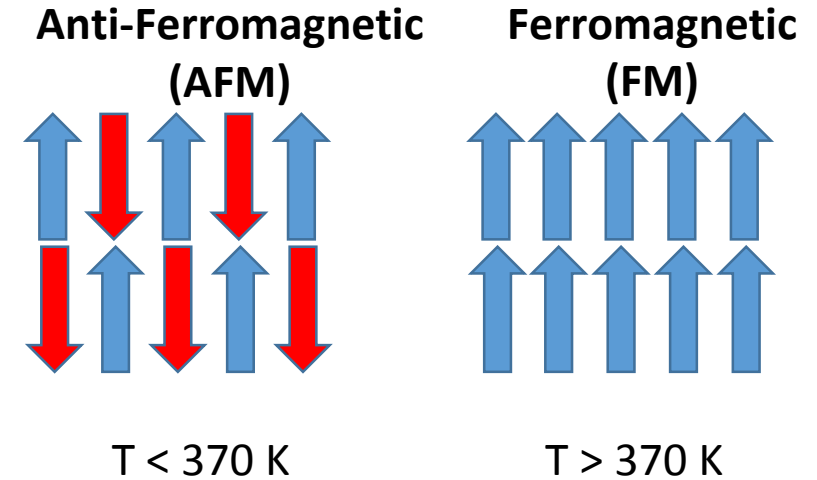
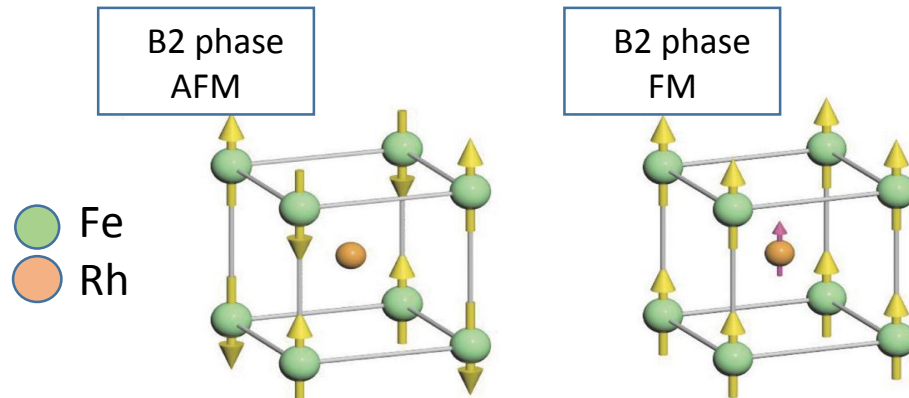
FeRh B2 phase, Pm-3m, a = 2.983Å

SrTiO₃ Pm-3m, a = 3.905Å



Iron Rhodium (FeRh)

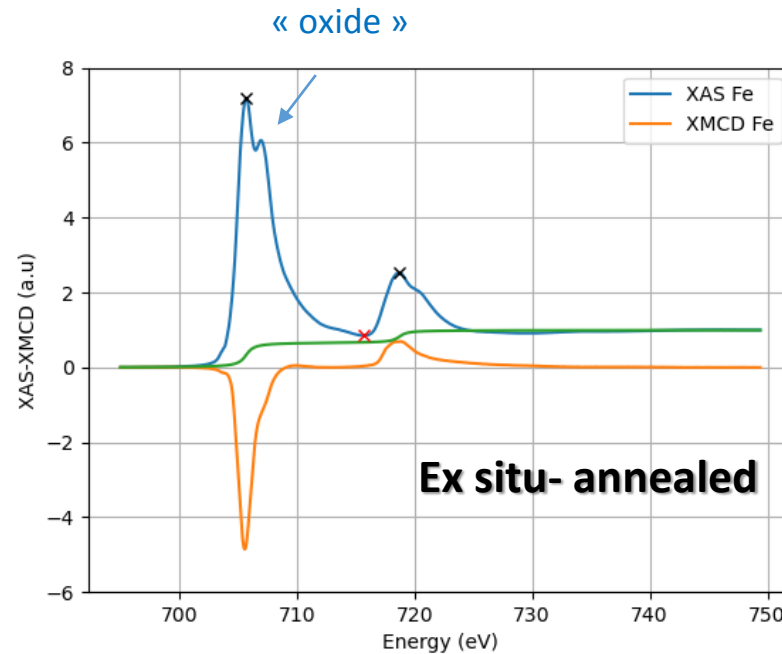
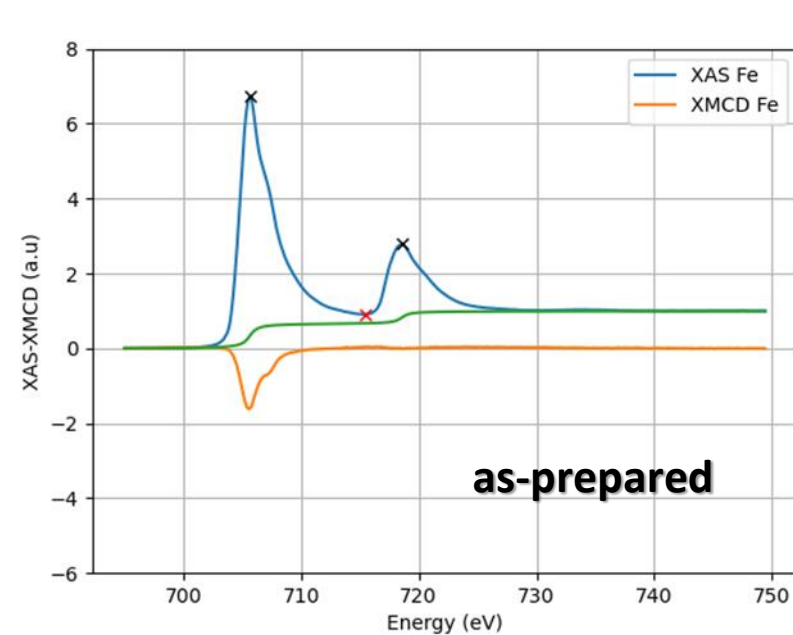
- FeRh bulk in the chemically ordered B2 phase presents metamagnetic transition: it is antiferromagnetic at temperatures lower than 370 K and ferromagnetic at higher temperatures.
- This metamagnetic transition happens along with a lattice parameter expansion.
- In thin film form, the B2 phase can be achieved after annealing at 700° C, presenting the metamagnetic transition.



Magnetic Properties of B2 FeRh NPs on perovskite

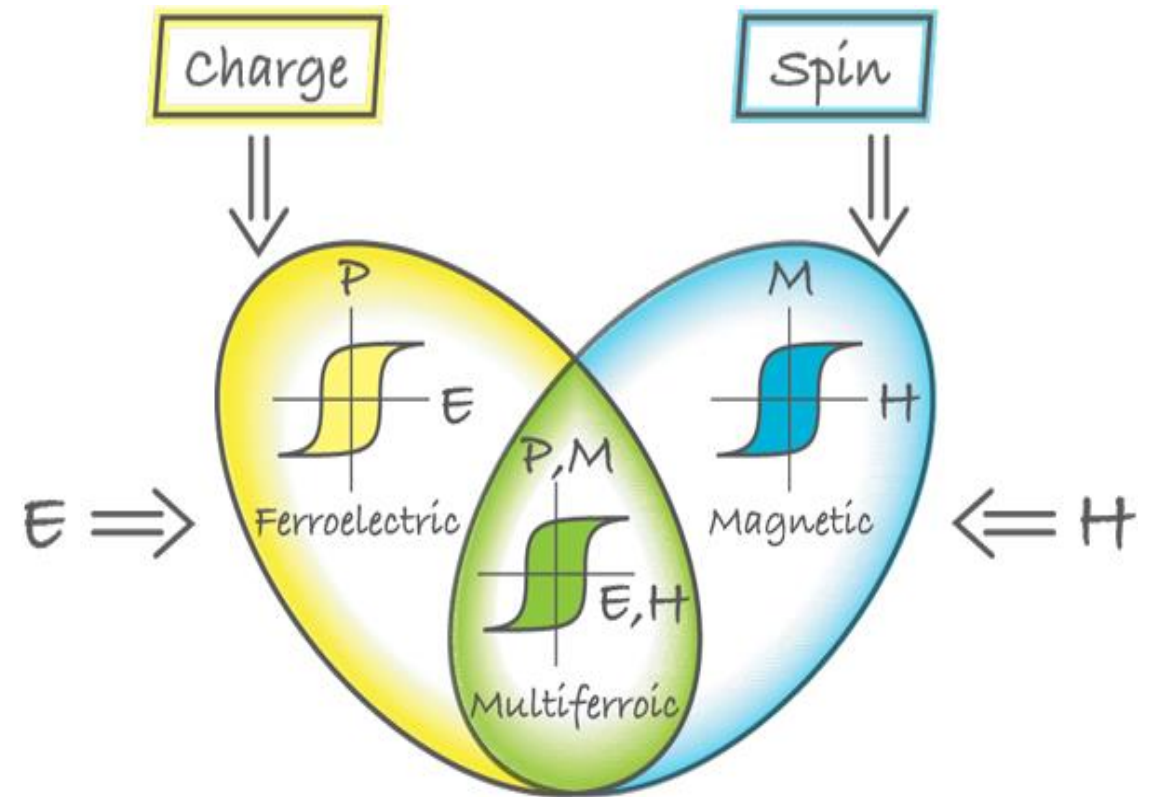
XAS/XMCD at Fe- $L_{2,3}$ edges as-prepared, after annealing and transfer in air

7nm-FeRh clusters on (001) BTO thin film on STO crystal



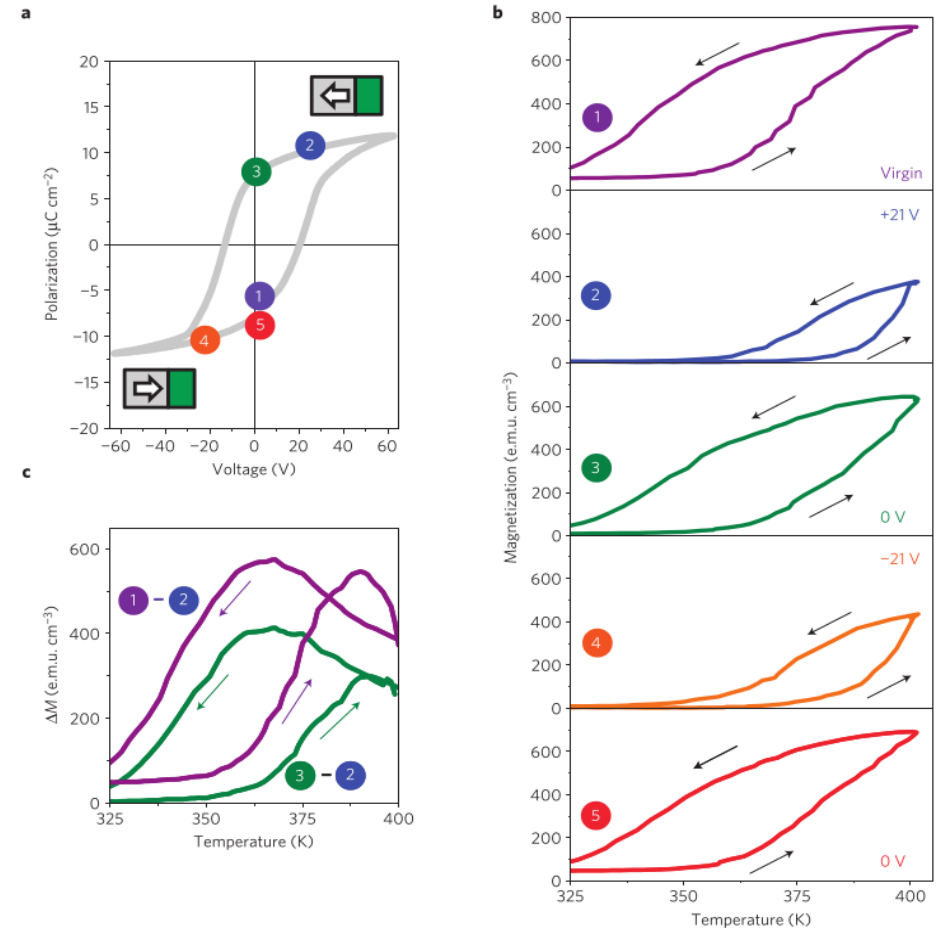
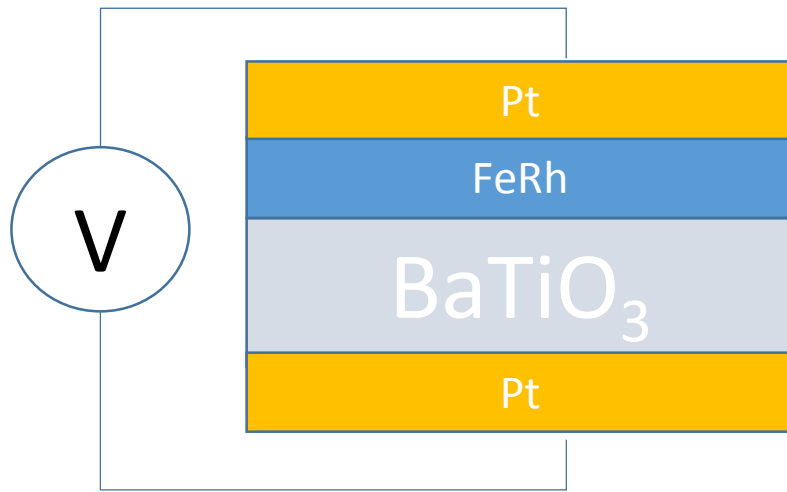
Hybrid multiferroic

- Hybrid multiferroic corresponds to a system that contains a Ferroelectric material and a Ferromagnetic material.
- FeRh metamagnetic transition can be controlled by other external stimuli not only by temperature.



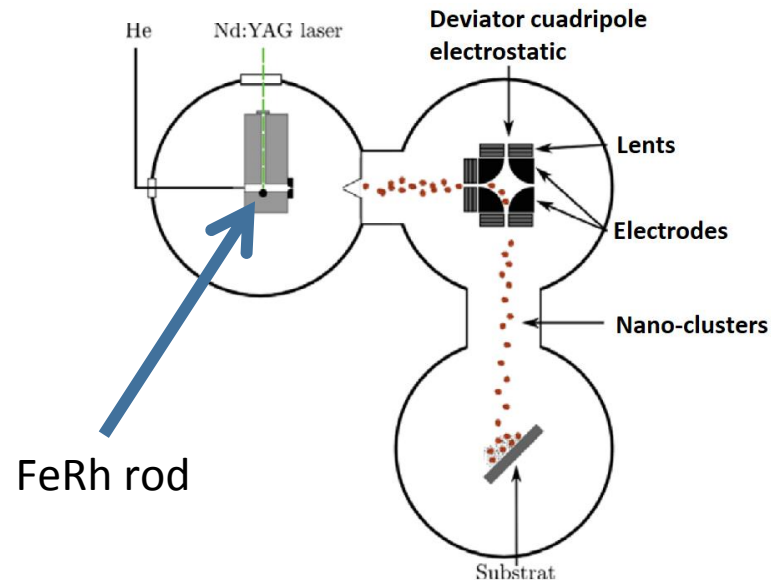
FeRh film over BaTiO₃

- It is possible to shift the transition temperature of FeRh layers over BaTiO₃ using voltage.
- SrTiO₃ is interesting because is similar to BaTiO₃.

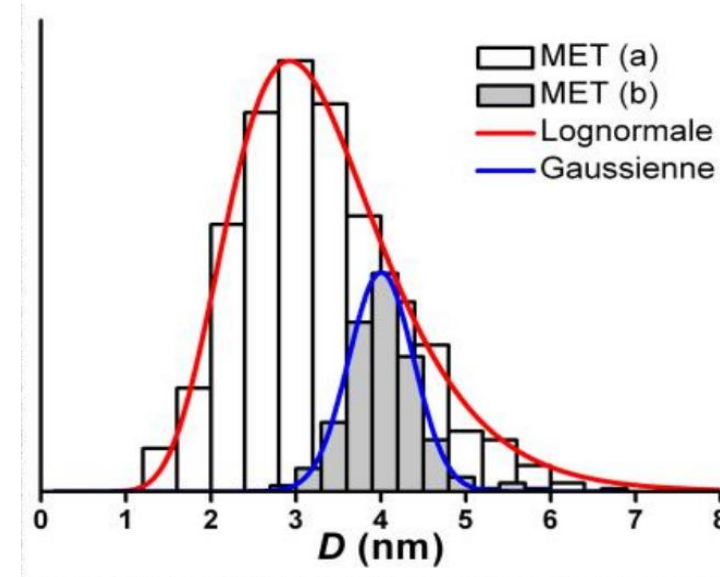


Sample preparation

- Low energy cluster beam deposition mass-selected.
- Pulsed laser heats an FeRh rod.
- Nanoparticles are formed in gas phase.
- Charged nanoparticles can be deviated using a quadrupole.



Scheme of the nano cluster deposition chamber



Size distribution for mass-selected (blue) and not mass selected (red)